Level Densities from Excitation Functions of Isolated Levels*

J. R. HUIZENGA†
University of Rochester, Rochester, New York 14627 and
Argonne National Laboratory, Argonne, Illinois 60439
H. K. VONACH‡
Technische Hochschule, München, Germany and Argonne National Laboratory, Argonne, Illinois 60439
AND
A. A. KATSANOS§, A. J. GORSKI, AND C. J. STEPHAN||
Argonne National Laboratory, Argonne, Illinois 60439

(Received 7 November 1968)

Thick-target excitation functions were measured for the reactions $Co^{59}(p, \alpha_0)Fe^{56}$, $Co^{59}(p, \alpha_1)Fe^{56}$, $Co^{59}(p, \alpha_2)Fe^{56}$, $Mn^{55}(p, \alpha_0)Cr^{52}$, $Mn^{55}(p, \alpha_1)Cr^{52}$, and $Ni^{62}(p, \alpha_0)Co^{59}$ at two or more angles for proton bombarding energies 6–13.5 MeV. The $Fe^{56}(\alpha, p_0)Co^{59}$ reaction was studied at α-particle bombarding energies of 12–18.5 MeV. These measurements were used to determine the parameters in three different level-density formulas which were thought to be reasonable candidates to describe the level densities of the residual nuclei. In addition, the experimental values of the cross sections to isolated levels were used in conjunction with available values of the level width Γ from cross-section fluctuation measurements to determine level densities of compound nuclei at about 20-MeV excitation energy. The absolute values and energy dependence of the nuclear level density in the excitation energy range 0–20 MeV investigated for several nuclei agree with a back-shifted Fermi gas model. The constant-temperature model gives a reasonable fit to the level density in the energy range 0–10 MeV but fails at higher excitation energies. The conventional shifted Fermi gas model does not reproduce the energy dependence and absolute values of the various experimental level densities for any value of the level-density parameter a.

I. INTRODUCTION

ABSOLUTE cross sections for formation of isolated residual levels in compound-nucleus reactions can be used for determination of nuclear level densities in two ways.

First, as pointed out by Ericson,[1] such measurements can be used to determine the values of the level density of the various residual nuclei formed in the reaction under consideration. As the cross section for formation of any particular level is governed by the competition of decay probability through this selected reaction channel to that for all other channels, the number of competing channels can be determined from the cross section of a single level. This number of effective competing reaction channels is directly related to the level densities of all the residual nuclei, the appropriate reaction Q values, and the transmission coefficients for the various emitted particles. Therefore, measurements of the absolute cross sections for isolated final levels as a function of bombarding energy give the energy dependence and absolute values of the level densities of the residual nuclei,[2] whereas the usual statistical analysis of the spectra of emitted particles gives only the energy dependence of the level density and not the absolute values. Furthermore, information about the spin cutoff factor σ of the residual nuclei can be obtained from the angular distributions of particles populating the isolated levels. Since the level density depends weakly on σ, it is necessary to determine this quantity only qualitatively. The determination of the level densities of residual nuclei is treated in Sec. III.

Second, absolute cross sections to isolated levels can be used in conjunction with available values of the level width Γ from cross-section fluctuation measurements to determine level densities of compound nuclei. This technique leads to an estimate of the nuclear level density at excitation energies in the neighborhood of 20 MeV.[3,4] The determination of the level densities of compound nuclei at these high excitation energies is treated in Sec. IV.

The purpose of the present paper is (a) to report some experimental measurements of excitation functions of reactions populating isolated levels; (b) to derive level densities from these and other data from the literature by the two methods discussed above, and (c) to test the validity of these methods in the energy range where other independent data on level densities are available.

II. MEASUREMENT OF EXCITATION FUNCTIONS

Excitation functions were measured for the reactions $Co^{59}(p, \alpha_0)Fe^{56}$, $Co^{59}(p, \alpha_1)Fe^{56}$, $Co^{59}(p, \alpha_2)Fe^{56}$, Fe^{56}-

* Work performed under the auspices of the U.S. Atomic Energy Commission.

† Present address: Nuclear Structure Research Laboratory, The University of Rochester, Rochester, N.Y. 14627.

‡ Present address: Physik Department, Technische Hochschule, München, Germany.

§ Present address: Centre d'Etudes Nucléaires de Saclay, Gif-sur-Yvette, France.

|| Present address: Laboratoire Joliot Curie, Département de Physique Nucléaire, Orsay (S and O), France.

[1] T. Ericson, Advan. Phys. **9**, 425 (1960).

[2] Preliminary values of the level density derived by this method were reported earlier by H. K. Vonach and J. R. Huizenga, Bull. Am. Phys. Soc. **9**, 168 (1964).

[3] H. K. Vonach and J. R. Huizenga, Phys. Rev. **138**, B1372 (1965).

[4] A. Richter, W. von Witsch, P. von Brentano, O. Häusser, and T. Mayer-Kuckuk, Phys. Letters **14**, 121 (1965).

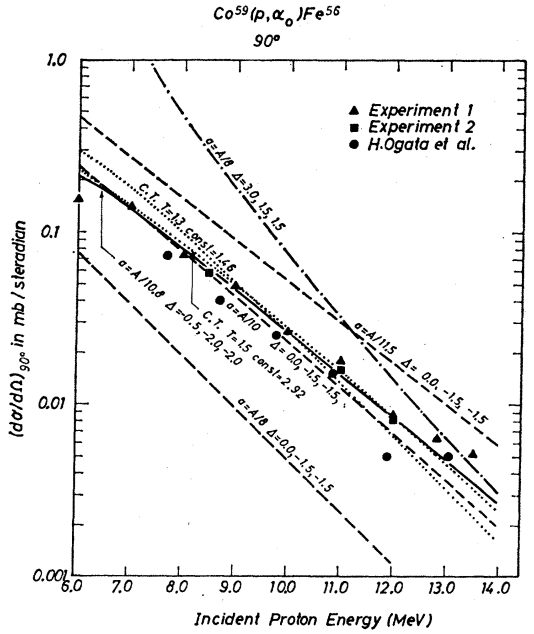

FIG. 1. Differential cross section (90°) as a function of proton bombarding energy for the $Co^{59}(p, \alpha_0)Fe^{56}$ reaction. The lines are theoretical calculations of the energy-dependent differential cross section [Eq. (1)] with various choices of the level-density parameters. The parameter a is the level-density parameter of Eq. (7). The values of Δ are given in the order Δ_α, Δ_p, and Δ_n, where these values correspond to an excitation energy shift in Eq. (7) for the residual nuclei formed by α, proton, and neutron emission, respectively. In this figure, these residual nuclei are Fe^{56}, Co^{59}, and Ni^{59}, respectively. Those lines identified by C. T. are constant-temperature calculations [Eq. (9)]. In the constant-temperature calculations, absolute values of Δ are not needed, only differences, such as $\Delta_n-\Delta_\alpha$, etc. The two types of level densities [Eqs. (7) and (9)] give equally good fits to the experimental data for the parameters $a=A/10.8$ MeV^{-1}, $\Delta_\alpha=-0.5$, $\Delta_p=-2.0$, and $\Delta_n=-2.0$ MeV [Eq. (7)] and $T=1.5$ MeV with a constant of 2.92 [Eq. (9)]. Experiments 1 and 2 were performed about 1 year apart and the results are shown as different symbols to indicate the degree of reproducibility.

$(\alpha, p_0)Co^{59}$, $Mn^{55}(p, \alpha_0)Cr^{52}$, $Mn^{55}(p, \alpha_1)Cr^{52}$, and Ni^{62}-$(p, \alpha_0)Co^{59}$ at two or more angles.

Protons and α particles accelerated in the Argonne tandem Van de Graaff were used to bombard metallic target foils of Co^{59}, Fe^{56}, Mn^{55}, and Ni^{62} of 1.0, 0.50, 0.77 and 0.96 mg/cm^2 thickness, respectively. Energy spectra of the emitted α particles were measured with surface-barrier detectors which were located 3–4 in. from the target. The bias on each solid-state detector was adjusted to give a response depth slightly greater than the range of the most energetic reaction α particle. With this operating condition, proton pulses were below 5 MeV. Deuterons and tritons were limited to energies less than 5 MeV by Q-value restrictions. The energy resolution of the detectors was about 50 keV. The experimental widths of the α peaks populating the ground and first excited levels are mainly due to the target thickness. Energy spectra of the emitted protons were measured with (dE/dX)-E solid-state counter telescopes in order to separate the protons from the α particles.

The experimental differential cross sections as a function of energy for several reactions are shown in Figs. 1–9. The total cross sections for the $Mn^{55}(p, \alpha_0)$ and $Mn^{55}(p, \alpha_1)$ reactions were calculated with the assumption of symmetry about 90° and the results are plotted in Fig. 6 along with the measurements of Ogata *et al.*[5] The absolute cross sections are believed to be accurate to about 10%. A large part of this error arises from the uncertainty in the effective target thickness (target thickness corrected for the angle between the target and the beam direction).

There are irregular fluctuations in some of the excitation functions shown in Figs. 1–9, especially those for the α_0 group at 170°. These irregularities are probably due to Ericson fluctuations which may be considerable even for thick targets (30–60 keV for the bombarding protons). The use of thicker targets makes it difficult to resolve the various α-particle groups. The dependence of the amplitude of the fluctuations on angle and spin of the final state, as well as the considerable damping of the fluctuations in the angle integrated cross sections (Fig. 6), agree qualitatively with fluctuation theory. However, these small fluctuations are unimportant to the over-all energy dependence of the excitation functions.

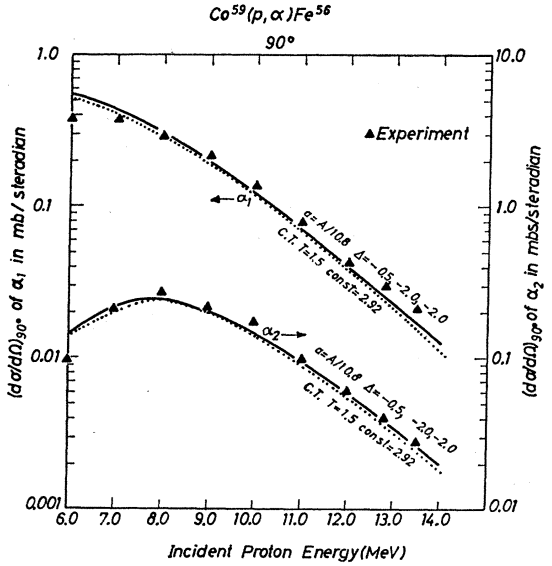

FIG. 2. Differential cross section (90°) as a function of proton bombarding energy for the $Co^{59}(p, \alpha_1)Fe^{56}$ and $Co^{59}(p, \alpha_2)Fe^{56}$ reactions. The points are experimental values and the lines represent theoretical values. Solid lines represent fits with Fermi gas calculations for $a=A/10.8$ MeV^{-1} and Δ_α, Δ_p, and Δ_n equal to -0.5, -2.0, and -2.0 MeV, respectively. The dashed lines are theoretical fits to the data with constant-temperature calculations. See caption of Fig. 1.

[5] H. Ogata, H. Itoh, Y. Masuda, K. Takamatsu, M. Kawashima, A. Masaike, and I. Kumahe, J. Phys. Soc. Japan 15, 1726 (1960).

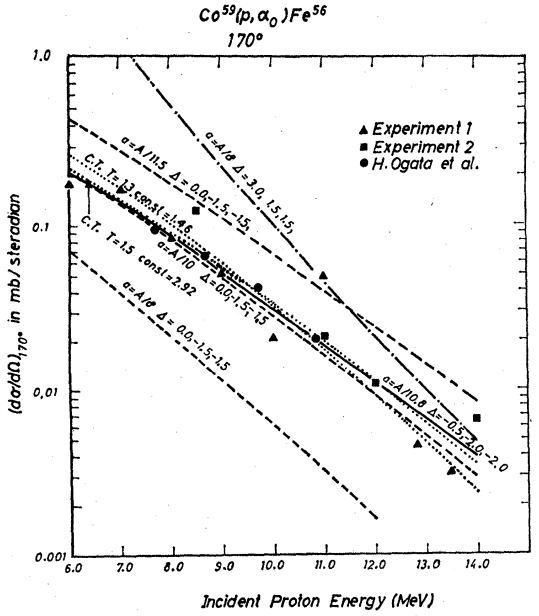

FIG. 3. Differential cross section (170°) as a function of proton bombarding energy for the $Co^{59}(p, \alpha_0)Fe^{56}$ reaction. Symbols have same meaning as Fig. 1.

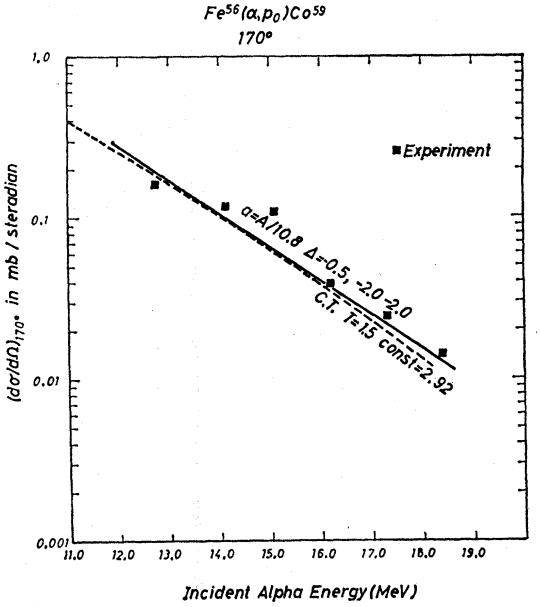

FIG. 5. Same as caption for Fig. 4 except the angle is changed to 170°.

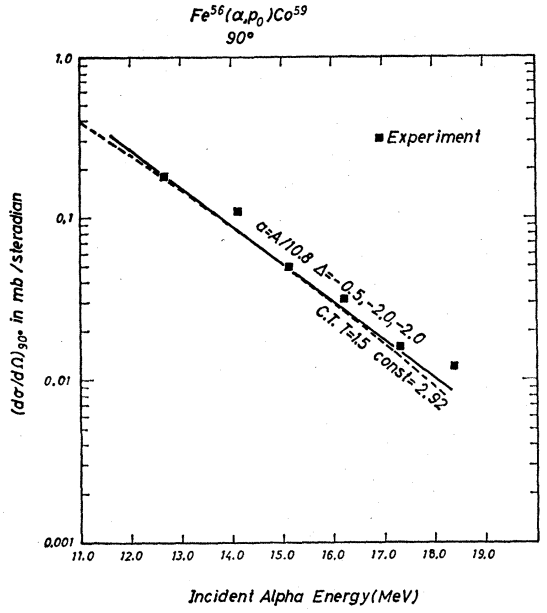

FIG. 4. Differential cross section (90°) as a function of α-particle bombarding energy for the $Fe^{56}(\alpha, p_0)Co^{59}$ reaction. The solid line represents a fit with a Fermi gas calculation for $a = A/10.8$ MeV^{-1} and $\Delta_\alpha(Fe^{56})$, $\Delta_p(Co^{59})$, and $\Delta_n(Ni^{59})$ equal to -0.5, -2.0, and -2.0 MeV, respectively. The dashed line is a fit with the constant-temperature theory for $T = 1.5$ MeV and a constant of 2.92.

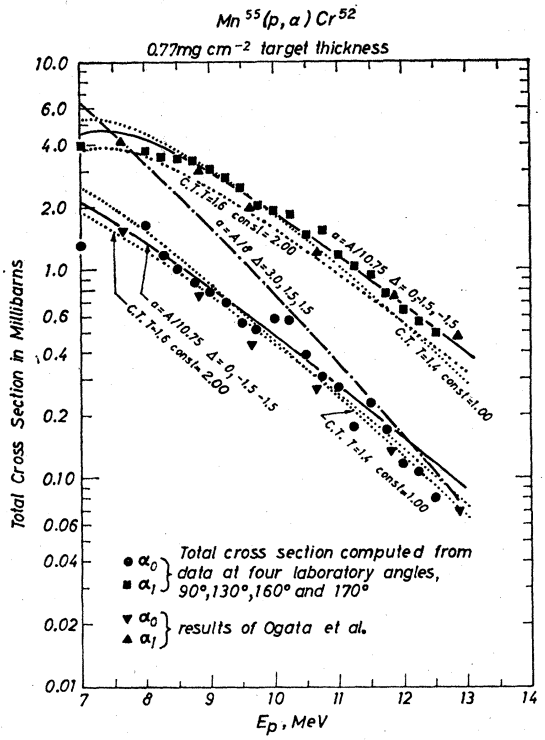

FIG. 6. Total cross section (in mb) as a function of proton bombarding energy for the $Mn^{55}(p, \alpha_0)Cr^{52}$ and $Mn^{55}(p, \alpha_1)Cr^{52}$ reactions. Theoretical cross sections for various level-density parameters are shown. Best agreement between experiment and theory is obtained for $T = 1.6$ MeV with the constant-temperature formalism and $a = A/10.75$ MeV^{-1} and Δ_α, Δ_p, and Δ_n equal to 0, -1.5, and -1.5 MeV, respectively, for the Fermi gas theory.

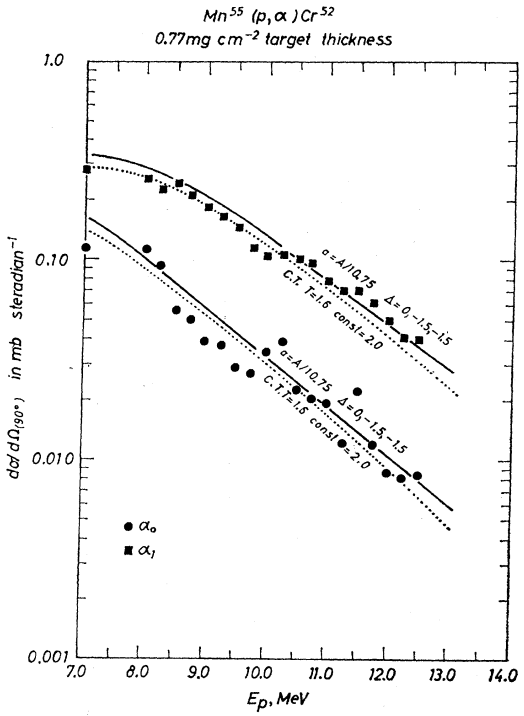

FIG. 7. Differential cross section (90°) as a function of proton bombarding energy for the $Mn^{55}(p, \alpha_0)Cr^{52}$ and $Mn^{55}(p, \alpha_1)Cr^{52}$ reactions. See caption of Fig. 6.

The exponential decrease in the cross section to an isolated final level with increasing energy is qualitatively in agreement with the prediction of compound-nucleus theory. The level densities of the residual nuclei are increasing exponentially, and hence the cross section to a particular final level decreases. If one corrects these excitation functions for the energy dependence of the total reaction cross section as well as the energy dependence of the transmission coefficients of the particles reaching the isolated level, an average temperature of the residual nuclei can be extracted from the excitation functions of Figs. 1–9. These temperatures agree qualitatively with those deduced by conventional methods. For example, in the $Mn^{55}(p, \alpha_0)$ and $Mn^{55}(p, \alpha_1)$ reactions a temperature of 1.4–1.6 MeV is deduced for Fe^{55} [most of the cross section is in the (p, n) reaction].

III. DETERMINATION OF LEVEL DENSITY AND SPIN CUTOFF FACTOR δ OF RESIDUAL NUCLEI

A. Theory

According to the statistical theory of nuclear reactions,[6] the differential cross section for a reaction $A(a, b)B$ at a fixed bombarding energy ϵ_1, which leads to a definite final state of angular momentum I_B, parity π_B, and excitation energy U_B in the residual nucleus B, can be expressed in the following way:

$$(d\sigma_{ab}/d\Omega)(I_B, \pi_B, U_B, \theta) = \sum_{L_{\text{even}}} A_L P_L(\cos\theta), \quad (1)$$

where

$$A_L = \frac{1}{4k_a^2(2I_A+1)(2I_a+1)} \sum_{S_1,l_1,S_2,l_2,J} \frac{\delta_n{}^m(-1)^{S_2-S_1} T_{al_1}(\epsilon_1) T_{bl_2}(\epsilon_2) Z(l_1 J l_1 J; S_1 L) Z(l_2 J l_2 J; S_2 L)}{G(J)}, \quad (2)$$

$$G(J) = \sum_{b'} \int_0^{U_{B'\,\max}} dU_{B'} \sum_{l_2'} T_{bl_2'}(\epsilon_2') \sum_{S_2'=|J-l_2'|}^{J+l_2'} \sum_{I_{B'}=|S_2'-I_{B'}|}^{S_2'+I_{B'}} \rho_{B'}(U_{B'}, I_{B'}, \pi_{B'}), \quad (3)$$

$$m = (-)^{l_1+l_2}, \quad (4)$$

$$n = \pi_1\pi_2, \quad (5)$$

and

$$U_{B'\,\max} = \epsilon_1 + Q_{ab'}. \quad (6)$$

The quantities I_A, I_a, J, I_B, and I_b are the spins of the target, projectile, compound nucleus, residual nucleus, and emitted particle, respectively; S_1 and S_2 are the channel spins in the incident and outgoing channels, respectively; l_1 and l_2 are the orbital angular momenta of the incident and outgoing particles, respectively; k_a is the wave number of the incident particles; $P_L(\cos\theta)$ is the Legendre polynomial of order L; $T_{al_1}(\epsilon_1)$ and $T_{bl_2}(\epsilon_2)$ are transmission coefficients for the projectile and the emitted particle, respectively, with total energies in the c.m. systems (channel energies) of ϵ_1 and ϵ_2; $Z(l_1 J l_1 J, S_1 L)$ and $Z(l_2 J l_2 J, S_2 L)$ are the so-called Z coefficients and are defined as sums of products of Racah and Clebsch-Gordan coefficients[6] (we make the random sign assumption which implies that L is even and that the angular distribution is symmetric about 90°). $\rho_{B'}(U_{B'}, I_{B'}, \pi_{B'})$ is the energy and spin-dependent density of levels of one parity of the residual nucleus formed by the emission of particle b' with channel energy ϵ_2', and the sum over b' refers to the sum over all the different types of emitted particles. The quantities π_1 and π_2 are the parities of the entrance

[6] A. C. Douglas and N. MacDonald, Nucl. Phys. 13, 382 (1959).

and exit channels, respectively. It should be emphasized that Eq. (1) is valid only for comparison with "thick-target" experiments, where the energy interval in the compound nucleus is large enough to completely damp the fluctuations and validate the random sign assumption.

As can be seen from Eqs. (1)–(3), the differential cross section of an isolated level in a single residual nucleus depends on the level densities of all residual nuclei formed in the interaction between a particular projectile and target. For the energies considered in this paper, only the residual nuclei formed by emission of neutrons, protons, and α particles need be considered. In some cases, one of the reactions (usually neutron emission) dominates and the level density of one particular nucleus is determined.

The transmission coefficients of the entrance and exit channels were calculated with an ABACUS II computer program. Optical-model parameters employed were those of Perey[7] for protons, Huizenga and Igo[8] for α particles, and Bjorklund and Fernbach[9] for neutrons.

B. Calculation of Excitation Functions for Various Level Densities

Calculations of the theoretical differential cross sections as a function of angle and projectile bombarding energy were performed with Eqs. (1)–(3) for different forms of the level density. In the calculation of the theoretical differential cross section, it is assumed that for each total angular momentum the formation and decay cross sections are independent of each other. Assuming the transmission coefficients of the entrance and exit channels are given by an optical model, the remaining unknowns in Eqs. (1)–(3) are the level densities of the residual nuclei. Different forms of the level densities of the residual nuclei were inserted into Eq. (3) and the level-density parameters of each of these different level-density equations were determined by optimizing each fit between the theoretical and experimental excitation functions. The following three forms of the level density were used.

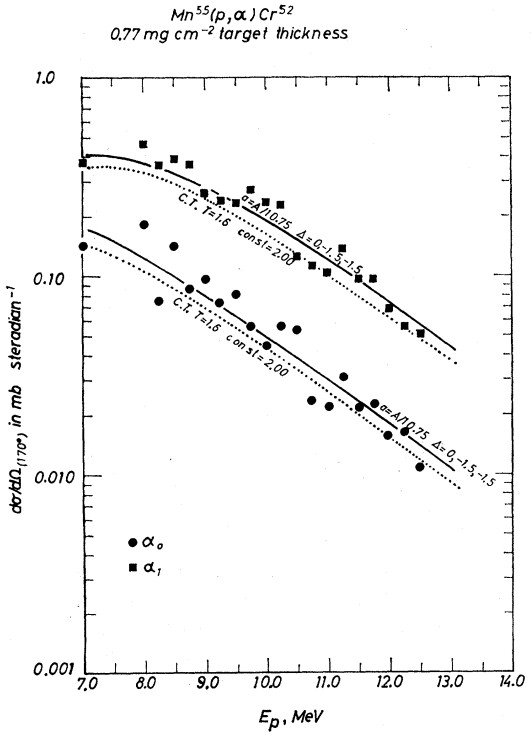

FIG. 8. Same as caption for Fig. 7 except the angle is changed to 170°.

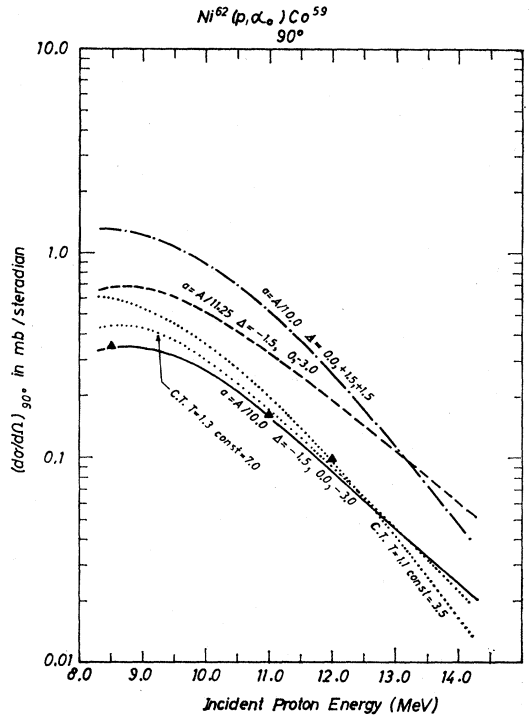

FIG. 9. Differential cross section (90°) as a function of proton bombarding energy for the $Ni^{62}(p, \alpha_0)Co^{59}$ reaction. The experimental data are reasonably well fitted with a Fermi gas calculation for $a=A/10$ MeV^{-1} and $\Delta_\alpha(Co^{59})$, $\Delta_p(Ni^{62})$, and $\Delta_n(Cu^{62})$ equal to -1.5, 0 and -3.0 MeV, respectively, and with a constant-temperature calculation for $T=1.3$ MeV and a constant of 7.0.

1. *Shifted Fermi Gas Level Density for Levels of Spin J and One Parity π at Excitation Energy U*

$$\rho(U,J,\pi)=\frac{(1/48\sqrt{2})\hbar^3 a^{1/2}(2J+1)}{\vartheta^{3/2}(U+t-\Delta)^2}$$

$$\times\exp\left[2a^{1/2}(U-\Delta)^{1/2}-\frac{J(J+1)}{2\sigma^2}\right], \quad (7)$$

where a, ϑ, t, and Δ are the level-density parameter, moment of inertia, thermodynamic temperature, and

[7] F. G. Perey, Phys. Rev. **131**, 745 (1963).
[8] J. R. Huizenga and G. Igo, Nucl. Phys. **29**, 462 (1962).
[9] F. Bjorklund and S. Fernbach, Phys. Rev. **109**, 1295 (1958).

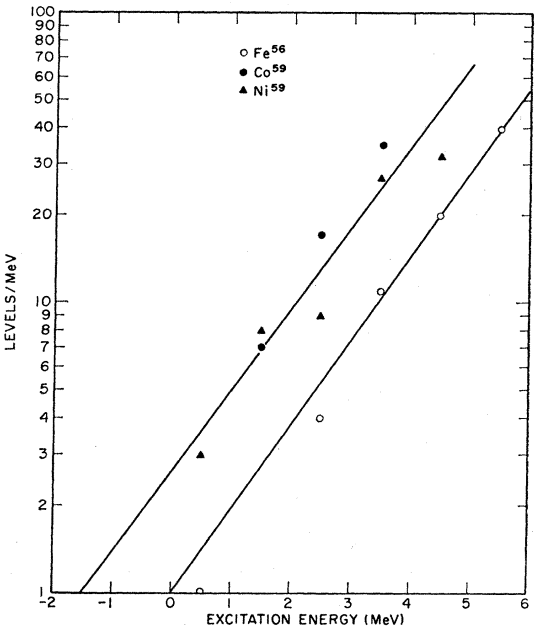

FIG. 10. Level density (levels/MeV) is plotted as a function of excitation energy, where the experimental data are obtained by counting of levels resolved with a magnetic spectrograph.

pairing energy parameter, respectively. The spin cutoff parameter $\sigma^2=\mathcal{I}t/\hbar^2$, where a nuclear radius of $1.2A^{1/3}$ F is assumed in the computation of $\mathcal{I}$. In the shifted Fermi gas model, the pairing energy is zero, Δ, and 2Δ for odd, odd-mass, and even nuclei, respectively (Δ is a positive quantity). Although this form of the level density seriously underestimates the level density at low excitation energies, it has been used frequently in statistical model calculations and results with this model are included to indicate its inadequacy.

2. *Back-Shifted Fermi Gas Level Density for Levels of Spin J and One Parity π at Excitation Energy U*

Again the level density is given by Eq. (7); however, the Fermi gas energy scale is shifted. In the limiting case, the Δ values are reduced by twice the energy difference between the odd and odd-mass nuclear surfaces such that Δ is now zero for even nuclei and correspondingly less for odd-mass and odd nuclei (negative values in both cases). In less extreme cases, Δ for even nuclei is still positive. This form of the level density has been proposed[10,11] as an empirical description of the level density over the whole energy range 0–20 MeV and seems to give a reasonable fit to experimental data over this energy range.[11]

[10] D. W. Lang and K. J. LeCouteur, Nucl. Phys. **14**, 21 (1959).
[11] A. A. Katsanos, Argonne National Laboratory Report No. ANL-7289, 1967 (unpublished).

3. *Constant-Temperature Level Density for Levels of Spin J and One Parity π at Excitation Energy U*

The level density of each residual nucleus b is given by

$$\rho_b(U,J,\pi)=c\frac{(2J+1)}{2\sigma^2}\times\exp\left[\frac{U+(\Delta_n-\Delta_b)}{T}-\frac{J(J+1)}{2\sigma^2}\right], \quad (8)$$

where $(\Delta_n-\Delta_b)$ is the energy difference in the Δ's of the nucleus formed by neutron emission and the nucleus formed by emission of particles of type b. This form of the level density requires only differences in Δ's; however, the constant c has to be determined from experimental data such as the known levels determined from magnetic spectrographs. The total level density of the residual nucleus formed by emission of particles b, $\rho_b(U)$, is given by

$$\rho_b(U)=2c\exp\{[U+(\Delta_n-\Delta_b)]/T\}, \quad (9)$$

where the constants c of Eqs. (8) and (9) are identical. The nuclear temperature T and the parameters $(\Delta_n-\Delta_b)$ and the constant can be estimated from experimental data as mentioned above and illustrated in Fig. 10. This form of the level density gives good fits to the experimental data in the low-excitation-energy region (0–10 MeV).

C. Results and Discussions of Calculations with Various Level Densities

Two kinds of calculations were performed with the above three forms of the nuclear level density. First, the various level-density parameters were varied with the assumption of a rigid-body moment of inertia in order to obtain the best agreement between the calculated and experimental excitation functions. Second, an estimate of the magnitude of the deviation from the rigid-body moment of inertia is obtained by comparison of the calculated and experimental angular distributions at particular energies with the above level-density parameters and a variable moment of inertia. To obtain the same absolute cross sections with, for example, a half-rigid-body moment of inertia, it is necessary to reduce slightly the level-density parameter a.

Comparisons of the experimental data with theoretical calculations based on a compound-nucleus mechanism for the assumption of a rigid-body moment of inertia are shown in Figs. 1–9. In Figs. 1 and 3, it is shown that the shifted Fermi gas level density (Sec. III B *1*) gives too steep a slope to the energy-dependent cross section. The values of Δ for the shifted Fermi gas level density for the residual nuclei are $\Delta_\alpha=3.0$ MeV (Fe^{56}), $\Delta_p=1.5$ MeV (Co^{59}), and $\Delta_n=1.5$ MeV (Ni^{59}). As the level-density parameter a is increased, the calculated cross sections are reduced but the energy dependence is entirely wrong.

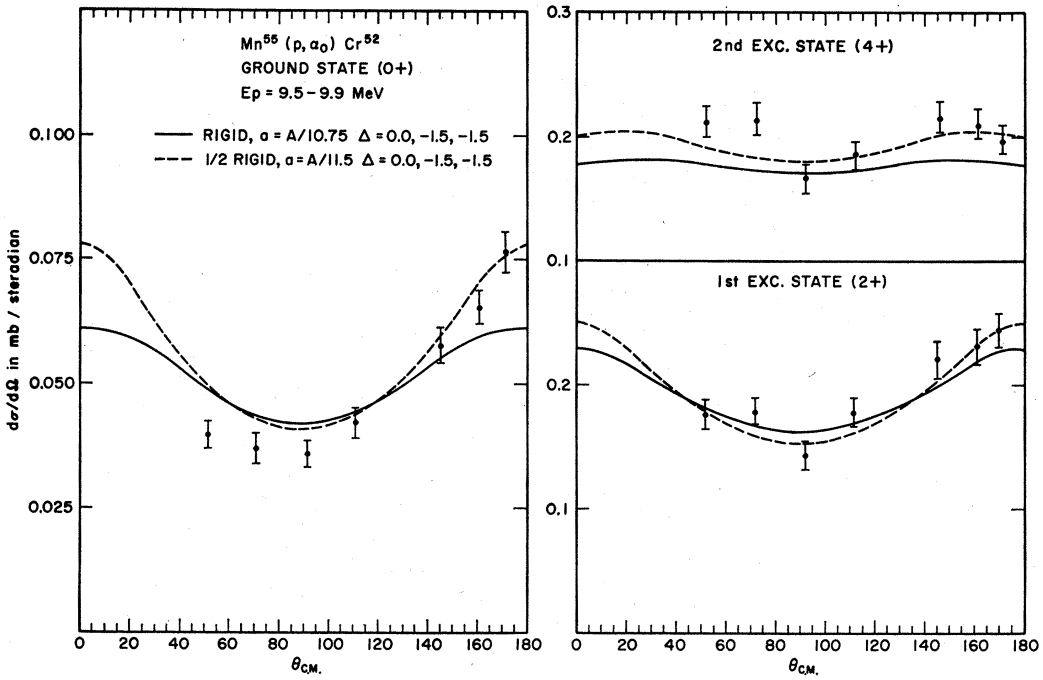

FIG. 11. Differential cross section as a function of angle for the $Mn^{55}(p, \alpha_0)Cr^{52}$, $Mn^{55}(p, \alpha_1)Cr^{52}$, and $Mn^{55}(p, \alpha_2)Cr^{52}$ reactions. The solid and dashed lines are theoretical fits for the Fermi gas model with rigid and half-rigid moments of inertia, respectively. The level-density parameters are those determined in previous figures.

The calculated cross sections and their energy dependence can be brought into agreement with experimental cross sections for the $Co^{59}(p, \alpha_0)$ reaction with either the back-shifted Fermi gas (Sec. III B *2*) or the constant-temperature level density (Sec. III B *3*) as shown in Figs. 1 and 3. The best fit with the back-shifted Fermi gas gives level-density parameters $a=A/10.8$, $\Delta_\alpha(Fe^{56})=-0.5$, $\Delta_p(Co^{59})=-2.0$, and $\Delta_n(Ni^{59})=-2.0$ MeV. An almost equivalent fit is obtained with a constant-temperature level density with $T=1.5$ and c of Eq. (9) equal to 2.92. As mentioned earlier, the constant-temperature level density requires only differences in Δ quantities, such as $\Delta_n-\Delta_\alpha$, and these differences are taken from the level-density plots directly as illustrated in Fig. 10. Several other less desirable fits are shown also in Figs. 1 and 3.

With the back-shifted Fermi gas [$a=A/10.8$, $\Delta_\alpha(Fe^{56})=-0.5$, $\Delta_p(Co^{59})=-2.0$ MeV, and $\Delta_n(Ni^{59})=-2.0$ MeV] and the constant-temperature level density ($T=1.5$ MeV), excellent agreement is obtained with the experimental data for the $Co^{59}(p, \alpha_1)$ and $Co^{59}(p, \alpha_2)$ reactions (Fig. 2) and the $Fe^{56}(\alpha, p_0)$ reaction (Figs. 4 and 5). Calculations with the other parameters shown in Figs. 1 and 3 again give unsatisfactory fits.

In Fig. 6, theoretical fits to the $Mn^{55}(p, \alpha_0)$ and $Mn^{55}(p, \alpha_1)$ reactions are shown. The best fits were obtained with the parameter $a=A/10.75$, $\Delta_\alpha(Cr^{52})=0.0$ MeV, $\Delta_p(Mn^{55})=-1.5$, and $\Delta_n(Fe^{55})=-1.5$ MeV for the back-shifted Fermi gas and $T=1.6$ MeV for the constant-temperature level density with $c=2.0$. Comparisons between calculation and experiment for the $Mn^{55}(p, \alpha_0)$ and $Mn^{55}(p, \alpha_1)$ reactions at 90° and 170° are shown in Figs. 7 and 8, respectively. In the constant-temperature model, there is some ambiguity in the determination of the temperature T and the constant c of Eq. (9). For example, the cross sections of Figs. 1–5 can be fit almost as well with $T=1.3$ and $c=1.46$ for Ni^{59} and the cross sections of Figs. 6–8 can be fit almost as well with $T=1.4$ and $c=1.0$ for Fe^{55}. Although the cross-section fits with these latter parameters are poorer, the agreement between the derived level densities and level count data are slightly better.

A comparison between experiment and theory for the $Ni^{62}(p, \alpha_0)$ reaction is shown in Fig. 9. The data are insufficient to draw any firm conclusions, although the back-shifted Fermi gas level density with $a=A/10.0$, $\Delta_\alpha(Co^{59})=-1.5$ MeV, $\Delta_p(Ni^{62})=0$, and $\Delta_n(Cu^{62})=-3.0$ MeV gives a reasonable fit to the three data points.

Angular distributions were calculated for the $Mn^{55}(p, \alpha_0)$, $Mn^{55}(p, \alpha_1)$, and $Mn^{55}(p, \alpha_2)$ reactions with full- and half-rigid-body moments of inertia. The level-density parameters were those obtained from the fitting of the excitation functions with the back-shifted Fermi gas. From Fig. 11, it can be seen that the experimental data favor a reduced moment of inertia. Angular distributions were calculated also for the $Cl^{37}(p, \alpha_0)$, $Cl^{37}(p, \alpha_1)$, and $Cl^{37}(p, \alpha_2)$ reactions with

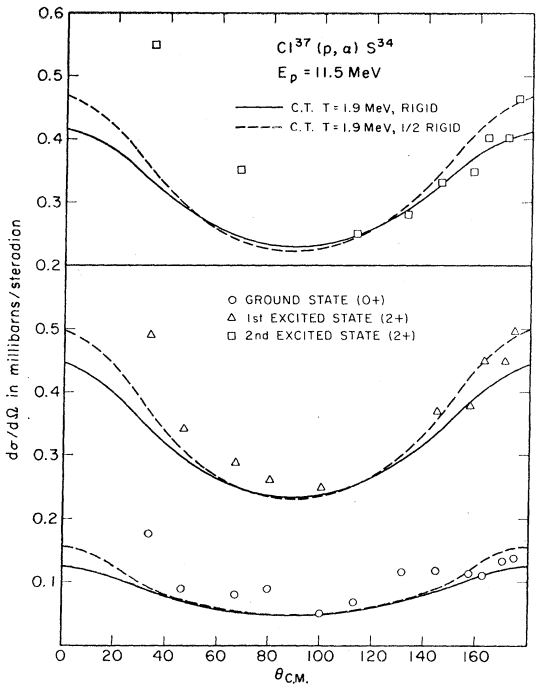

FIG. 12. Differential cross section as a function of angle for the $Cl^{37}(p, \alpha_0)S^{34}$, $Cl^{37}(p, \alpha_1)S^{34}$, and $Cl^{57}(p, \alpha_2)S^{34}$ reactions (see Ref. 12). Solid and dashed lines are theoretical fits to the experimental data with the constant-temperature model for rigid and half-rigid moments of inertia.

full- and half-rigid-body moments of inertia. In Fig. 12, the calculations are compared with experimental measurements.[12] Although no quantitative determination of the moment of inertia is possible from the data of Figs. 11 and 12, its value appears to range between the rigid-body value and a half-rigid value or slightly less. As mentioned earlier the level density is rather insensitive to the moment of inertia, and we calculate the level density for two values of the moment of inertia, the rigid and half-rigid values.

The $Cl^{37}(p, \alpha)$ reactions were studied[12] at a single bombarding energy. A constant-temperature-type level density was assumed with the constants adjusted to fit the values of the level density of the most important residual nucleus Ar^{37}. The levels of this nucleus are known up to 7 MeV from high-resolution magnetic spectrograph measurements.[13]

The fact that the moment of inertia may be reduced to one-half the rigid-body moment does not change significantly our conclusions about the energy dependence of the level density which was derived by comparing calculated and experimental excitation functions with a rigid moment of inertia. In Fig. 13, we show that equally good agreement between calculated and experimental excitation functions is obtained with a half-rigid moment of inertia when the level-density parameter a is reduced by 6%.

IV. DETERMINATION OF COMPOUND-NUCLEUS LEVEL DENSITY

A. Theory

The quantity $G(J)$ in Eq. (3) is related to the total width Γ_J and average spacing $D_{J,\pi}$ of the compound levels at excitation energy U_C by[14]

$$\Gamma_J = (D_{J,\pi}/2\pi)G(J), \tag{10}$$

where

$$D_{J,\pi} = \frac{D_{0,\pi}}{(2J+1)\exp[-J(J+1)/2\sigma_C^2]} \tag{11}$$

and $D_{0,\pi}$ is the spacing of zero spin levels of one parity and σ_C is the spin cutoff factor of the compound nucleus at excitation energy U_C. Substitution of Eqs. (2), (10), and (11) into Eq. (1) gives

$$\frac{d\sigma_{ab}}{d\Omega}(I_B, \pi_B, U_B, \theta) = \frac{\lambda_a^2}{8\pi(2I_A+1)(2I_a+1)} \sum_{S_1,l_1,S_2,l_2,J,L} \frac{D_{0,\pi}\delta_n{}^m(-1)^{S_2-S_1}T_{al_1}(\epsilon_1)T_{bl_2}(\epsilon_2)Z_1Z_2P_L(\cos\theta)}{\Gamma_J(U_C)(2J+1)\exp[-J(J+1)/2\sigma_C^2]}. \tag{12}$$

If the quantity $\Gamma_J(U_C)$ is replaced by an averaged value Γ, it may be removed from the summation over J giving the following equation:

$$\frac{d\sigma_{ab}}{d\Omega}(I_B, \pi_B, U_B, \theta)\frac{\Gamma}{D_{0,\pi}} = \frac{\lambda_a^2}{8\pi(2I_A+1)(2I_a+1)} \sum_{S_1,l_1,S_2,l_2,J,L} \frac{\delta_n{}^m(-1)^{S_2-S_1}T_{al_1}(\epsilon_1)T_{bl_2}(\epsilon_2)Z_1Z_2P_L(\cos\theta)}{(2J+1)\exp[-J(J+1)/2\sigma_C^2]}. \tag{13}$$

The width Γ is now defined as a weighted average over the width Γ_J of the various compound spin states as described in Sec. IV B. The weighting factors are define as the fractional contributions of the various compound spin states to the cross section for the final state under consideration. These weighting factors, and therefore Γ, are, in principle, dependent on excitation energy, angle θ, and the spin and parity of the final state. It will be shown, however, that the dependence of Γ on these parameters is very weak. By use of Eq. (13), the spacing of zero spin levels $D_{0,\pi}$ in the compound nucleus can be calculated from differential cross sections to isolated levels if both the average width Γ and spin cutoff factor σ_C of the compound levels are known. Thus, these two quantities will be considered in more detail in the following sections.

The level density of the compound nucleus is deter-

[12] W. von Witsch, P. von Brentano, T. Mayer-Kuckuk, and A. Richter, Nucl. Phys. **80**, 394 (1966).

[13] C. H. Holbrow, P. V. Hewka, J. Wiza, and R. Middleton, Nucl. Phys. **79**, 505 (1966).

[14] T. Ericson, Ann. Phys. (N.Y.) **23**, 390 (1963), Eq. A3.4.

mined in Sec. IV in contrast to the level densities of the residual nuclei determined in Sec. III. In this section, we assume that we know the quantity Γ in Eq. (13) from other experimental measurements. The right-hand side of Eq. (13) is calculable once optical-model transmission coefficients are chosen for all the entrance and exit channels. The differential cross sections on the left-hand side of Eq. (13) are measured, leaving only the parameter $D_{0,\pi}$ (which is directly related to the level density of the compound nucleus) to be determined.

B. Dependence of Γ_J on J and Excitation Energy U_C

The J and energy dependence of the width Γ_J are calculated with Eq. (10) by substituting the value of $G(J)$ from Eq. (3) and assuming some form for the level densities of the compound and residual nuclei. As described in Sec. III B, the shifted and back-shifted Fermi gas level densities and a "modified constant-temperature" level density were used in Eqs. (10) and (3). The procedure for calculating Γ_J with the "modified constant-temperature" formalism is similar to that reported[3] previously where the level densities of the residual nuclei are decomposed into a constant term $\rho_n(U_C-B_n)$ and exponential terms with constant temperature [see Eq. (3) of Ref. 3]. In the "modified constant-temperature" formalism the absolute magnitude of Γ_J depends on the evaluation of $\rho_n(U_C-B_n, I_B=0,\pi)/\rho_C(U_C, J=0,\pi)$ which we have computed with the three forms of the level density described in Sec. III B. Plots of Γ_J as a function of J and excitation energy U_C are shown in Fig. 14 for the back-shifted Fermi gas model.

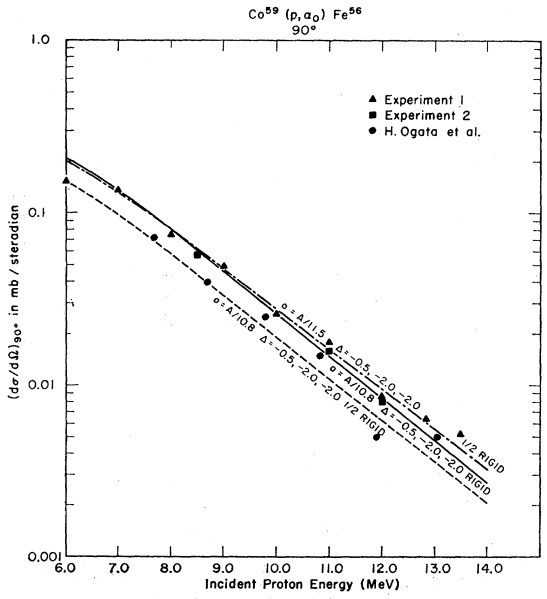

FIG. 13. Differential cross section (90°) as a function of proton bombarding energy for the $Co^{59}(p, \alpha_0)Fe^{56}$ reaction. Fermi gas theoretical fits illustrate the small change in a when the moment of inertia is changed from a rigid to a half-rigid value.

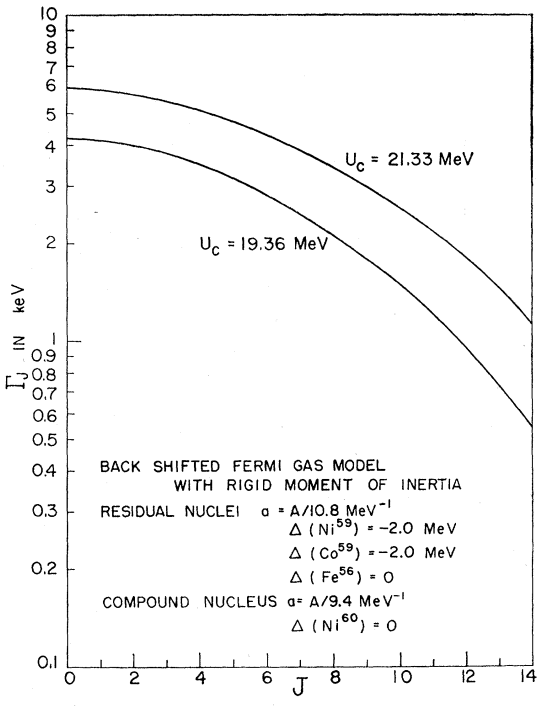

FIG. 14. Spin dependence of the total energy-level width Γ_J of Ni^{60} at two excitation energies. The solid lines were calculated using the back-shifted Fermi gas level densities with the parameters given in the figure.

C. Spin Cutoff Factor σ_C of Compound Nuclei

As already pointed out in Sec. IV A, the spin cutoff factor σ_C of the compound nucleus is needed for a calculation of $D_{0,\pi}$ from the differential cross sections and the average level width Γ. Previously it was proposed[4,12] that σ_C can be determined from experimental angular distributions of cross sections to isolated final levels according to Eq. (12). However, it can be seen from Eq. (1) that the differential cross section $d\sigma_{ab}(I_B, \pi_B, U_B, \theta)/d\Omega$ is independent of σ_C. The apparent dependence of the differential cross section on σ_C in Eq. (12) is, in fact, cancelled by the concealed σ_C dependence of Γ_J according to Eq. (10). Therefore, no methods are available presently for direct determination of σ_C at the excitation energies under consideration.

In the mass region of the nuclei investigated in this paper, the moment of inertia derived from σ determinations at lower excitation energies is equal to or larger than half the rigid-body moment. Hence, it seems safe to assume the same for the higher energies, and to perform the calculations with σ_C values corresponding to one-half-rigid and rigid-body moments of inertia. The uncertainty in the moment of inertia introduces an uncertainty in the average spacing of zero spin levels of one parity $D_{0,\pi}$ from Eq. (13). However, the compound-nucleus level density is calculated according to

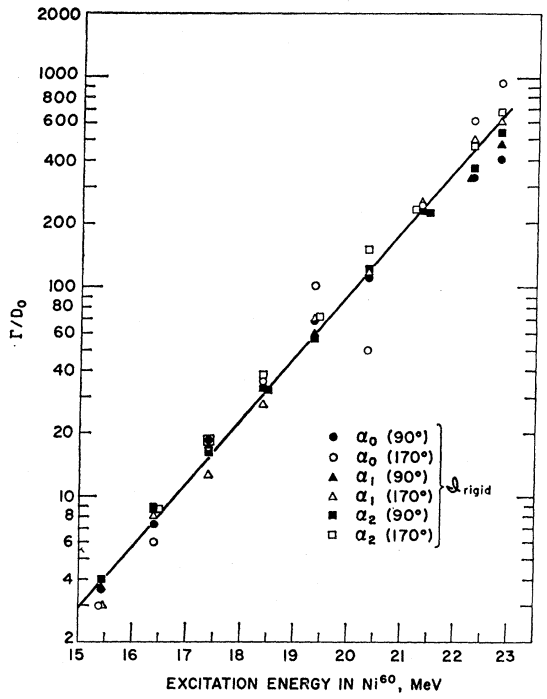

FIG. 15. The ratio Γ/D_0 as a function of excitation energy for Ni^{60}. The points are calculated from Eq. (13) and the relation $\Gamma/D_0=2\Gamma/D_{0,\pi}$. The right-hand side of Eq. (13) is first computed and then divided by the experimental differential cross section which appears on the left-hand side of Eq. (13). The calculation uses the rigid moment of inertia for evaluating σ_C.

the relation

$$\rho_C=2\sigma_C^2/D_0, \tag{14}$$

where ρ_C and D_0 are the level density and spacing, respectively, for both parities. The direct σ_C dependence of Eq. (14) cancels to a large extent the σ_C dependence of D_0. Therefore, the over-all uncertainty in ρ_C due to a lack of knowledge of σ_C is small and in most cases less than 30%.

D. Calculation of Level Width to Spacing Ratio Γ/D_0 from (p, α) Excitation Functions

The right-hand side of Eq. (13) depends on the quantum numbers I_B and π_B of the populated level in the residual nucleus, transmission coefficients of the entrance and exit channels, and the spin cutoff factor σ_C of the compound nucleus. As information exists on all of these quantities (see Sec. IV C), it is possible to evaluate the right-hand side of Eq. (13). The quantity Γ/D_0 ($\Gamma/D_0=2\Gamma/D_{0,\pi}$) can then be computed as a function of excitation energy U_C if measurements of $d\sigma_{ab}/d\Omega$ (I_B, π_B, U_B, θ) are available as a function of c.m. bombarding energy ϵ_1. The excitation energy U_C and the channel energy ϵ_1 are related by

$$U_C=\epsilon_1+Q_{a,\gamma}, \tag{15}$$

where $Q_{a,\gamma}$ is the energy release caused by the capture of particle a.

Such calculations of Γ/D_0 were performed for several reactions for which absolute cross sections were available from either the present measurements (Sec. II) or the literature. Two sets of calculations were performed using different values for the moment of inertia of the compound nucleus, viz., one-half-rigid and rigid-body moments of inertia. The calculations were performed with a CDC 3600 computer.[15] The multiple summations were performed for l_1 and $l_2\leq 17$, S_1 and $S_2\leq 14$, $J\leq 17$, and $L\leq 12$. The same transmission coefficients were used as in the residual nuclei level-density calculations.

The values of Γ/D_0 for compound nuclei Ni^{60} and Fe^{56} are shown as a function of excitation energy for both rigid- and half-rigid-body moments of inertia in Figs. 15–17. Although the individual values of Γ/D_0 show some scatter (see Sec. II in which the incomplete averaging of Ericson fluctuations is discussed), there is no systematic deviation between the Γ/D_0 values determined from data for different final states and angles. This indicates that the dependence of Γ on the exact form of the weighting functions used to determine it as an average over Γ_J is rather small. The weighting functions associated with the $0+(\alpha_0)$ and $4+(\alpha_2)$ states are considerably different; however, in spite of this, there is no evidence for a significant difference in Γ/D_0. In Figs. 15 and 16, the values of Γ/D_0 calculated for the 90° data at the two highest excitation energies

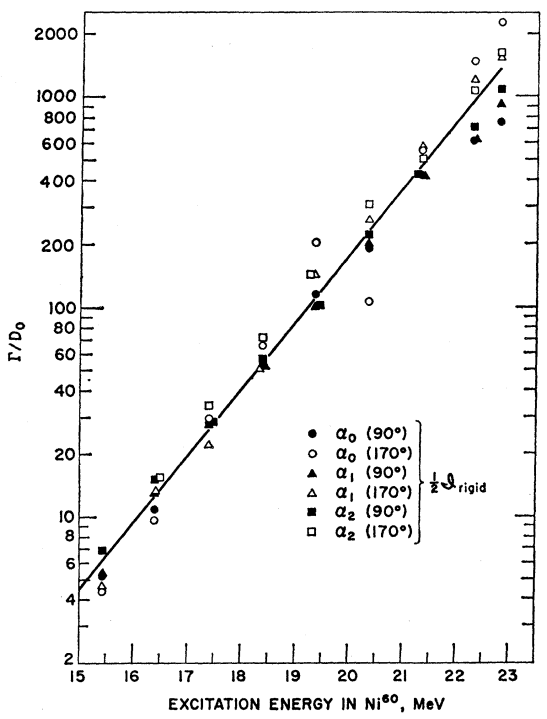

FIG. 16. Same as caption of Fig. 15 except the half-rigid moment of inertia is used to evaluate σ_C.

[15] The computer programs used for the statistical model calculations were modifications of a program initially developed by Dr. M. Halbert and Dr. H. Bowsher.

are smaller than those from the 170° data. This may be ascribed to a greater direct reaction contribution at 90°, although it seems unlikely that the results are substantially in error on account of a large fraction of the differential cross section being due to direct reaction. In Sec. II, it was shown that both the absolute cross sections to isolated levels and their energy dependence as well as angular distributions agree with the compound-nucleus character of these reactions.

E. Calculation of Level Density $\rho(U)$ of Compound Nucleus at High Excitation Energy

The quantities $D_0(U)$ and $\rho(U)$ can be calculated from the values of $\Gamma/D_0(U)$ determined in the previous section if independent knowledge of the level width Γ as a function of U is available. Determination of the width Γ_{fluct} from cross-section fluctuation measurements have been reported[11,12] for the reactions for which Γ/D_0 values were calculated. However, Γ was determined at only one energy. Therefore, two questions arise in attempting to calculate $\rho(U)$. First, how accurate is the assumption that the widths Γ_{fluct}, determined from fluctuations analyses, are equal to the widths of Eq. (10)? Second, how accurately can the energy dependence of Γ be predicted?

As already mentioned, Γ is defined as a weighted average over the Γ_J distribution according to the relation

$$1/\Gamma=(\sum_J P_J/\Gamma_J)/\sum_J P_J \tag{16}$$

with

$$P_J=\sum_{S_1,l_1,S_2,l_2,L}\frac{\delta_n{}^m(-1)^{S_2-S_1}T_{al_1}(\epsilon_1)T_{bl_2}(\epsilon_2)Z_1Z_2P_L(\cos\theta)}{(2J+1)\exp[-J(J+1)/2\sigma_C{}^2]}. \tag{17}$$

Similarly, the level width Γ_{fluct} determined from an autocorrelation function (derived from a fluctuating cross-section excitation function) is also a weighted average over Γ_J with weighting factors very similar to those given above.[16] The quantity Γ_{fluct} is related approximately to Γ_J by the following relation:

$$1/\Gamma_{\text{fluct}}{}^2\approx(\sum_J P_J'/\Gamma_J{}^2)/\sum_J P_J', \tag{18}$$

where P_J' is given by

$$P_J'=\sum_{S_1,l_1,S_2,l_2}\exp[J(J+1)/2\sigma_C{}^2]T_{al_1}{}^2(\epsilon_1)T_{bl_2}{}^2(\epsilon_2). \tag{19}$$

Expression (18) is valid only for angle integrated cross sections. However, if Γ_{fluct} is independent of angle θ, as is the case for all reactions considered here, Eq. (18) is expected to hold for differential cross sections also.

Comparison of Eqs. (16) and (17) with (18) and (19) shows that the weighting is performed in a similar way for the Γ calculated in the ratio Γ/D_0 and for the experimentally determined Γ_{fluct} if both correspond to the same final state. It should be noted that the weighting functions for the same type of Γ for two final states differing markedly in spin are less similar than the weighting factors P_J and P_J' for the same final state. As already mentioned, no significant differences in Γ/D_0 for Ni^{60} were found for the (0+) ground state and the (4+) second excited state in the $Co^{59}(p,\alpha)$ reactions (see Fig. 15). Within experimental error the same width Γ_{fluct} was obtained for the compound nuclei Ni^{60} and Fe^{56} from each of the (p,α_0) and (p,α_2) reactions. Hence, it is assumed that the errors due to the differences in Eqs. (16) and (18) and the associated different weighting factors P_J and P_J' are small compared to the experimental errors in Γ_{fluct} and $d\sigma_{ab}/d\Omega$. An alternative way to derive Eq. (13) is to assume that Γ_J in Eq. (12) is independent of J.

The second question on the energy dependence of Γ is more difficult since the energy dependence of the width Γ can be calculated only if the compound-nucleus level density is already known. However, the energy dependence of Γ is very weak compared to that of $D_0(U)$

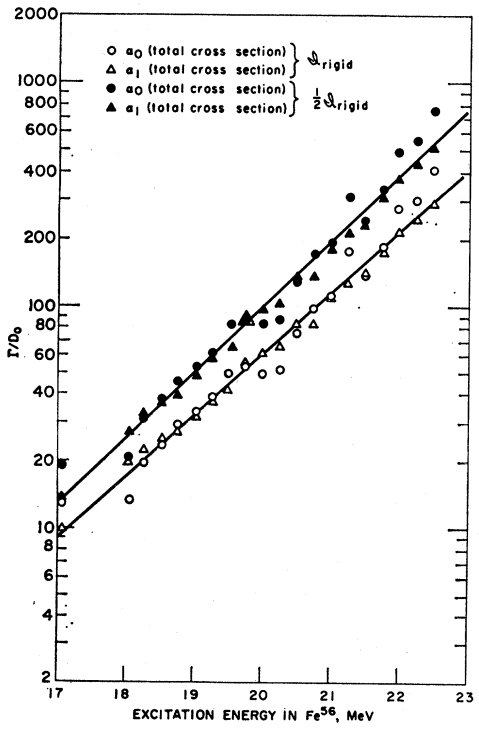

FIG. 17. The ratio Γ/D_0 as a function of excitation energy for Fe^{56}. See caption of Fig. 15.

[16] E. Gadioli, I. Iori, A. Marini, and M. Sansoni, Nuovo Cimento **44B**, 338 (1966).

TABLE I. Summary of reactions, bombarding energy ranges, and

Reaction	Spin and parity of final state	Angle of measurement (deg)	Bombarding energy range in MeV	Residual nuclei and their excitation energy ranges: α-particle emission, Residual nucleus	α-particle emission, Maximum E^* (MeV)	Proton emission, Residual nucleus	Proton emission, Maximum E^* (MeV)	Neutron emission, Residual nucleus	Neutron emission, Maximum E^* (MeV)
$Co^{59}(p, \alpha_0)Fe^{56}$	0+	90, 170	6–13.5	Fe^{56}	9.1–16.5	Co^{59}	5.9–13.3	Ni^{59}	4.0–11.4
$Co^{59}(p, \alpha_1)Fe^{56}$	2+	90, 170	6–13.5	Fe^{56}	9.1–16.5	Co^{59}	5.9–13.3	Ni^{59}	4.0–11.4
$Co^{59}(p, \alpha_2)Fe^{56}$	4+	90, 170	6–13.5	Fe^{56}	9.1–16.5	Co^{59}	5.9–13.3	Ni^{59}	4.0–11.4
$Fe^{56}(\alpha, p_0)Co^{59}$	$\frac{7}{2}-$	90, 170	12–19	Fe^{56}	11.2–17.7	Co^{59}	8.0–14.5	Ni^{59}	6.1–12.6
$Mn^{55}(p, \alpha_0)Cr^{52}$	0+	90, 130, 160, 170	7–13	Cr^{52}	9.5–15.3	Mn^{55}	6.9–12.8	Fe^{55}	5.9–11.8
$Mn^{55}(p, \alpha_1)Cr^{52}$	2+	90, 130, 160, 170	7–13	Cr^{52}	9.5–15.3	Mn^{55}	6.9–12.8	Fe^{55}	5.9–11.8
$Ni^{62}(p, \alpha_0)Co^{59}$	$\frac{7}{2}-$	90	8–12	Co^{59}	8.2–12.2	Ni^{62}	7.9–11.8	Cu^{62}	3.6–7.1
$Cl^{37}(p, \alpha_0)S^{34}$	0+	Several	11.5	S^{34}	14.2	Cl^{37}	11.2	Ar^{37}	9.6
$Cl^{37}(p, \alpha_1)S^{34}$	2+	Several	11.5	S^{34}	14.2	Cl^{37}	11.2	Ar^{37}	9.6
$Cl^{37}(p, \alpha_2)S^{34}$	2+	Several	11.5	S^{34}	14.2	Cl^{37}	11.2	Ar^{37}	9.6

or $\rho(U)$. Therefore, the energy-dependent level density can be determined rather accurately even though the energy dependence of Γ is derived from rather inaccurate first estimates of $\rho(U)$.

The following procedure was adopted in the calculations. First, values of $\Gamma_J(U)$ were computed as a function of energy according to Eq. (10) using estimates of the level densities of the compound and residual nuclei as determined in the first part of this paper. A weighed average of Γ_J was normalized to the experimental value of Γ_{fluct} at the corresponding excitation energy. From these energy-dependent values of $\Gamma(U)$ and the values of $\Gamma/D_0(U)$ discussed earlier, values of $\rho_C(U)$ were derived from Eq. (14). The resulting values of $\rho_C(U)$ as a function of excitation energy are plotted for Fe^{56}, Ni^{60}, and Ar^{38} in Figs. 18–20, respectively. It should be emphasized that one point near 20 MeV in both Fig. 18 and Fig. 19 is based on an experimental value of the width Γ. The other high-energy points require a calculated energy dependence of Γ. Since the energy dependence of Γ is insensitive to the form of the level density chosen, the error introduced into these other values of the high-energy level density from this source is of the order of a factor of 2. The level-density values plotted at the lower energies are from direct level counts for Fe^{56},[17] Ni^{60},[18] and Ar^{38}.[19] In addition, a value of the level density at 10 MeV is plotted for Ar^{38}. This value is derived from the density of 1− resonances[20] at this excitation energy, in conjunction with the level-density parameters $a=4.8$ MeV^{-1} and $\Delta=1.5$ MeV in the back-shifted Fermi gas model with a rigid-body moment of inertia.

The energy-dependent level density is fitted with an equation of the form of that given by Eq. (7); however, the total level density is given by $\rho(U)=2\sigma^2\rho(U, J=0)$. The back-shifted Fermi gas level density gives the best fit to the low- and high-excitation-energy data. For the even nuclei Fe^{56}, Ni^{60}, and Ar^{38}, values of the param-

[17] A. A. Katsanos, J. R. Huizenga, and H. L. Vonach, Phys. Rev. **141**, 1053 (1966); G. Brown and S. E. Warren, Nucl. Phys. **77**, 365 (1966); H. K. Vonach and J. R. Huizenga, Phys. Rev. **149**, 844 (1966).

[18] C. H. Paris, Massachusetts Institute of Technology Laboratory for Nuclear Science Annual Progress Report, 1958, p. 117 (unpublished); R. G. Tee and A. Aspinall, Nucl. Phys. **A98**, 417 (1967).

[19] R. G. Allas, L. Meyer-Schützmeister, and D. von Ehrenstein, Nucl. Phys. **61**, 289 (1965).

[20] P. M. Endt and C. Van der Leun, Nucl. Phys. **A105**, 282 (1967).

the respective residual nuclei and their level-density parameters.

Level-density parameters of residual nuclei

Fermi gas a (MeV^{-1})	Δ_α (MeV)	Δ_p (MeV)	Δ_n (MeV)	$\mathcal{I}$	Constant temperature Constant	T (MeV)	$\Delta_n-\Delta_\alpha$ (MeV)	$\Delta_n-\Delta_p$ (MeV)	$\mathcal{I}$	Most important residual nucleus
$A/10.8$	−0.5	−2.0	−2.0	Rigid	2.92	1.5	−1.5	0	Rigid	Ni^{59}
$A/11.5$	−0.5	−2.0	−2.0	½Rigid	1.46	1.3	−1.5	0	Rigid	Ni^{59}
$A/10.8$	−0.5	−2.0	−2.0	Rigid	2.92	1.5	−1.5	0	Rigid	Ni^{59}
					1.46	1.3	−1.5	0	Rigid	Ni^{59}
$A/10.8$	−0.5	−2.0	−2.0	Rigid	2.92	1.5	−1.5	0	Rigid	Ni^{59}
					1.46	1.3	−1.5	0	Rigid	Ni^{59}
$A/10.8$	−0.5	−2.0	−2.0	Rigid	2.92	1.5	−1.5	0	Rigid	Ni^{59}
					1.46	1.3	−1.5	0	Rigid	Ni^{59}
$A/10.75$	0	−1.5	−1.5	Rigid	2.00	1.6	−1.4	0.6	Rigid	Fe^{55}
					1.00	1.4	−1.4	0.6	Rigid	Fe^{55}
$A/10.75$	0	−1.5	−1.5	Rigid	2.00	1.6	−1.4	0.6	Rigid	Fe^{55}
					1.00	1.4	−1.4	0.6	Rigid	Fe^{55}
$A/11.4$	−1.5	0	−3.0	Rigid	7.00	1.3	−1.4	−2.8	Rigid	Cu^{62} and Ni^{62}
					0.90	1.9	−1.7	0	Rigid	Ar^{37}
					0.45	1.6	−1.7	0	Rigid	Ar^{37}
					0.90	1.9	−1.7	0	Rigid	Ar^{37}
					0.45	1.6	−1.7	0	Rigid	Ar^{37}
					0.90	1.9	−1.7	0	Rigid	Ar^{37}
					0.45	1.6	−1.7	0	Rigid	Ar^{37}

eter Δ of Eq. (7) of 0–1.5 MeV give the best fit to the data.

V. COMPARISON OF LEVEL DENSITIES DERIVED FROM EXCITATION FUNCTIONS WITH OTHER DATA

In Table I, we summarize the reactions, bombarding energy ranges, and the respective residual nuclei which were investigated. The level-density parameters which give good fits to the experimental data are included also. In most of these reactions, neutron emission is the most important decay mode of the compound nuclei. For Ni^{60}, Fe^{56}, and Ar^{38}, the difference between the proton and neutron binding energies is considerably less than the Coulomb barrier and the residual nuclei formed by both neutron and proton emission are of odd-mass type; hence, neutron emission predominates. In the decay of the compound nucleus Cu^{63}, proton and neutron emission are of about equal importance due to the large negative Q value for the $Ni^{62}(p, n)$ reaction.

The cross section for a particular level is determined approximately by the competition between the decay probability to the specific level under consideration and the total decay probability for neutron emission. This latter probability is a function of the level density of the residual nucleus formed by neutron emission. Since neutron emission predominates, the calculated excitation functions are more sensitive to the choice of level-density parameters for the residual nuclei reached by neutron emission than for residual nuclei reached by other processes. The comparison of theoretical and experimental excitation functions give, therefore, chiefly information about the level-density parameters of the residual nuclei formed by neutron emission.

The individual levels of Ni^{59},[21] Fe^{55},[22] and Ar^{37} [13,23] are known up to several MeV of excitation energy from high-resolution magnetic spectrograph measurements of (d, p) and other reactions. In addition, for Ni^{59} and Fe^{55}, the density of s-wave neutron resonances ($\frac{1}{2}+$ levels) is known at the neutron binding energy.[24] In

[21] E. R. Cosman, C. H. Paris, A. Sperduto, and H. A. Enge, Phys. Rev. **142**, 673 (1966).

[22] *Nuclear Data Sheets*, compiled by K. Way *et al.* (Printing and Publishing Office, National Academy of Sciences—National Research Council, Washington, D.C. 20025, 1959), NRC 59-2-19.

[23] P. M. Endt and C. Van der Leun, Nucl. Phys. **A105**, 260 (1967).

[24] E. G. Bilpuch, K. K. Seth, C. D. Bowman, R. H. Tabony, R. C. Smith, and H. W. Newson, Ann. Phys. (N.Y.) **14**, 387 (1961); C. D. Bowman, E. G. Bilpuch, and H. W. Newson, *ibid.* **17**, 319 (1962).

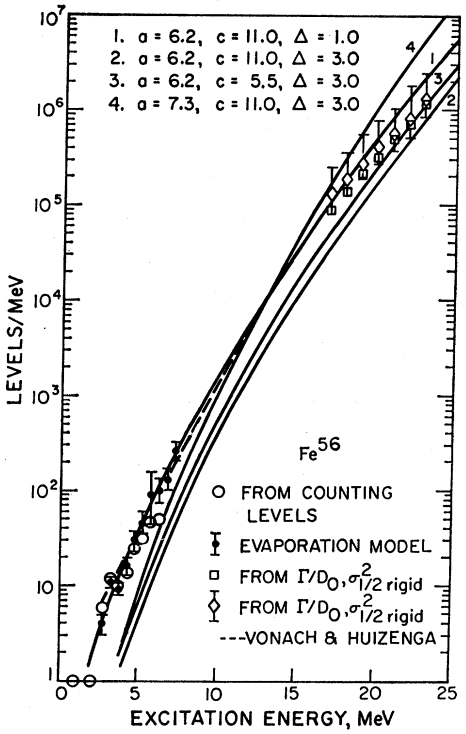

FIG. 18. Level density (levels/MeV) of Fe^{56} as a function of excitation energy. The lines are theoretical Fermi gas calculations with the given parameters, where a is the level-density parameter and c is the moment of inertia divided by $\hbar^2$. The two values of c correspond to rigid and half-rigid moments of inertia.

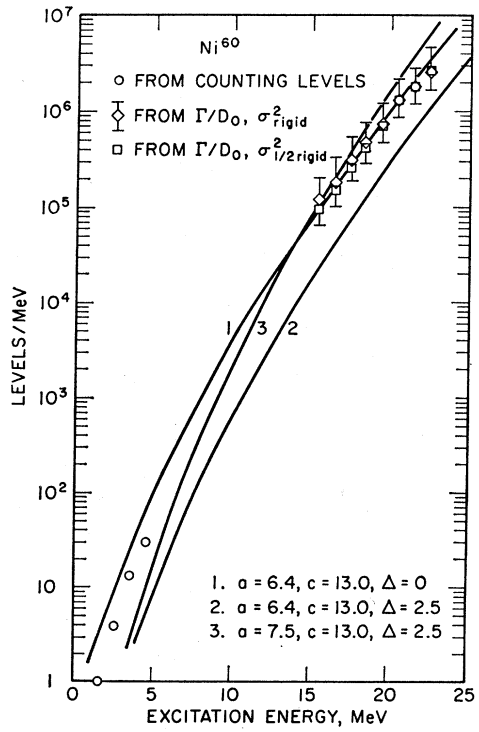

FIG. 19. Level density (levels/MeV) of Ni^{60} as a function of excitation energy. See caption of Fig. 18.

Figs. 21–23 the level densities derived from excitation functions (Sec. III) are compared with level densities obtained by direct level counting and neutron resonance data. The level densities calculated with the conventional shifted Fermi gas model are shown also.

The conventional shifted Fermi gas model underestimates the level densities at lower excitation energies. The constant-temperature model and the back-shifted Fermi gas model give similar level densities over a limited energy range up to about 10 MeV, which explains the fact that about equally good fits to the excitation functions are obtained with both models. However, there is a general tendency for the level densities derived from our cross-sections data to be

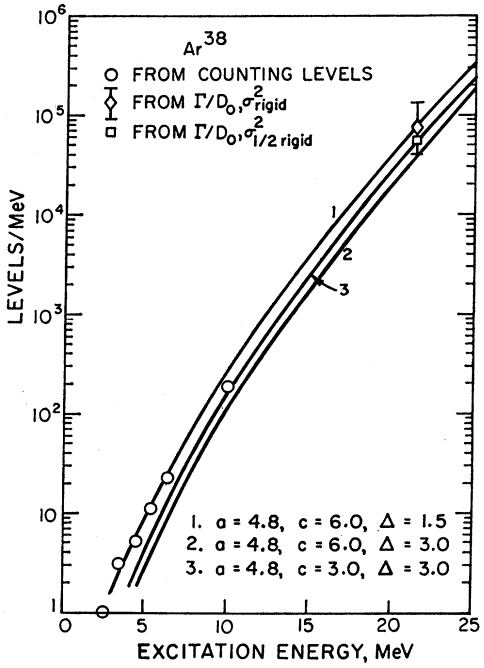

FIG. 20. Level density (levels/MeV) of Ar^{38} as a function of excitation energy. See caption of Fig. 18.

larger than the level densities derived from neutron resonance and level count data. For Fe^{55}, the discrepancy with the resonance data is within experimental error and the slight discrepancy with the level count data may be caused by missed levels in the $Fe^{54}(d, p)$ experiment. Although the level density of Ar^{37} from level count data is smaller than that from cross-section data, no final conclusions can be drawn from this case since the absolute cross section was measured at only one energy. In addition, the cross-section information determines the Ar^{37} level density in the 7–10-MeV excitation energy range which is a few MeV in excess of the level count data.

The level density of Ni^{59} determined from the absolute cross-section measurements is about a factor of 2 larger than the level count and resonance data. This

discrepancy is outside the combined errors of the experimental data and raises some question about the reliability of either one or both methods for determination of level densities.

If it is assumed that the level count and resonance data are correct for Ni^{59}, then the experimental absolute cross sections to isolated levels for this case are too small. Direct reaction contributions to these cross sections cause a discrepancy in the opposite direction. Cross sections that are too small require either a special hindrance factor (beyond the normal statistical theory) for particle emission to these isolated levels or a compound-nucleus–formation cross section which is only a

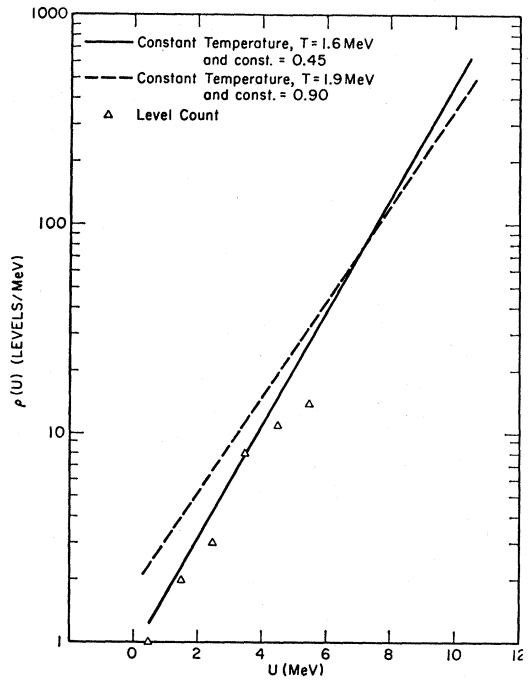

FIG. 21. Level density (levels/MeV) of Ar^{37} as a function of excitation energy. The constant-temperature lines are computed with Eq. (9).

fraction of the absorption cross section. Neither of these explanations are very satisfactory.

On the other hand, if the level density from the isolated level cross-section data is assumed correct, then one must explain why the resonance data gives a level density too small by a factor of 2. One possibility might be that there is a paucity of $\frac{1}{2}+$ levels in the vicinity of the neutron binding energy of Ni^{59} caused by special nuclear-structure effects. Then the observed resonance spacing is a poor indicator of the total level density which was assumed to be equal to $2\sigma^2\rho(\frac{1}{2}+)$.

Unfortunately, it is not possible to resolve the discrepancy at present. More experimental data are needed. If the latter explanation is correct, one might expect that only a few nuclei would have anomolous $\frac{1}{2}+$ level densities and, hence, the discrepancy in level densities

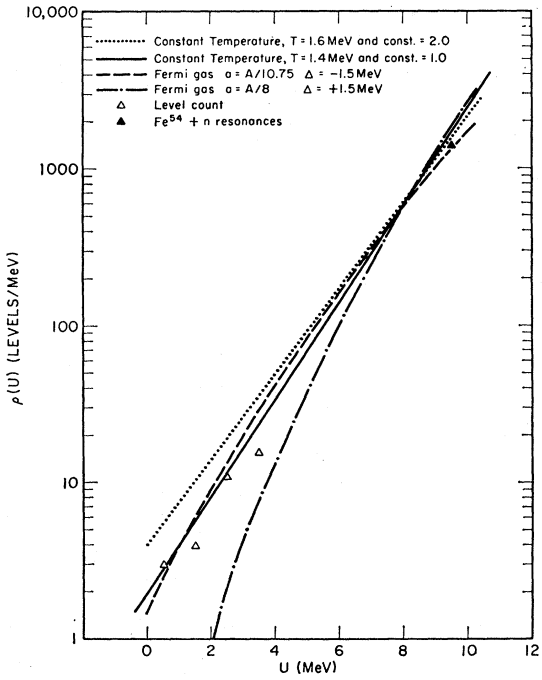

FIG. 22. Level density (levels/MeV) of Fe^{55} as a function of excitation energy. Constant-temperature lines are computed with Eq. (9) and Fermi gas lines with Eq. (7) summed over all J values. The $Fe^{54}+n$ resonance point is calculated with $2\sigma^2=34.4$ (derived from $U-\Delta=at^2-t$ with $a=A/10.75$, and rigid-body moment of inertia with $r_0=1.2$ F).

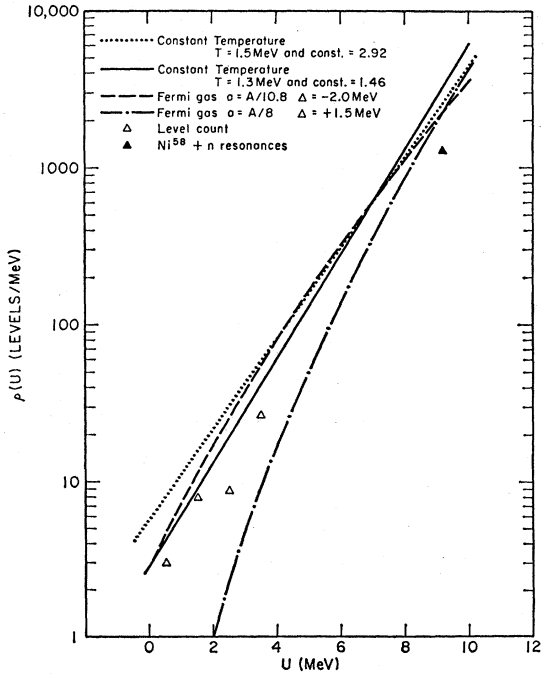

FIG. 23. Level density (levels/MeV) of Ni^{59} as a function of excitation energy. The $Ni^{58}+n$ resonance point is calculated with $2\sigma^2=37.4$. See caption of Fig. 22.

by the different methods would be limited to these nuclei. If one of the former explanations is valid, one expects a general disagreement of level-densities derived from cross sections to isolated levels and resonance data. Measurements of cross sections for neutron emission to isolated levels should be made also to compare with the reported charged-particle emission.

The uncertainty in the level densities of the residual nuclei discussed in the above paragraphs affects also the values of the level densities of the compound nuclei. The compound-nucleus level densities plotted in Figs. 18–20 are based on the level densities of the residual nuclei derived from absolute cross sections. If it turns out that the smaller level densities from the resonance and level count data are more accurate, the high-energy level densities would have to be reduced by factors of up to 2. This accounts for the present compound level densities of Fe^{56} and Ni^{60} being larger than earlier values[3] which were based on residual nucleus level densities from s-wave resonance spacings. However, these uncertainties in level densities make only a small change in the level-density parameters a and Δ.

VI. CONCLUSIONS

The present analysis of level densities of some nuclei in the mass region of $A=35$–60 indicates that the back-shifted Fermi gas model gives an adequate description of both the absolute values and the energy dependence of the nuclear level density over the investigated energy range 0–20 MeV. The constant-temperature model gives a reasonable fit to the experimental data in the energy range 0–10 MeV but fails at higher excitation energies. The conventional shifted Fermi gas model does not give a satisfactory fit to the experimental level densities for any value of the level-density parameter a. This result is in agreement with recent analyses of level densities by Gadioli and Zetta[25] who also apply a shift in the excitation energy.

The fictitious ground state for an odd A nucleus described by a Fermi gas model is expected to be located below the actual ground state if one assumes nondegenerate single-particle levels and a pairing interaction of the BCS type.[26] However, except for deformed nuclei, the single-particle levels, i.e., the subshells of the spherical shell model, are $2I+1$-fold degenerate. The effect of this degeneracy on the nuclear level density has been investigated theoretically by Bloch[27] and Rosenweig.[28] These authors show that the level density is still described approximately by the Fermi gas model with a shifted ground state. The magnitude of the energy shift of the ground state due to the degeneracy of the subshells depends on the number of nucleons in the unfilled subshells. For nuclei some distance from closed shells, this energy shift is of about the same magnitude as, and opposite in direction to, the energy shift caused by the pairing interaction. Neither of these energy shifts can be calculated very accurately at present. Hence, values of the energy shift of the ground state must be extracted from accurate measurements of absolute level densities over extended regions of excitation energy.

Values of the level-density parameter a and energy shift of the ground state Δ vary from nucleus to nucleus. The values of a for the even nuclei Fe^{56} and Ni^{60} are larger than the corresponding quantity for the odd-mass nuclei Fe^{55} and Ni^{59}. It is not possible to say at this time whether this is a general effect or whether it is localized to particular nuclei or regions of nuclei. The values of a derived from evaporation spectra have tended to be larger than those derived in this paper. However, when the large uncertainties in the value of a derived from spectra for the particular nuclei in question here are considered, the differences appear to be within allowable uncertainties.

The determination of level densities of residual nuclei from measurements of absolute cross sections of isolated levels is not restricted to excitation energies below the neutron binding energy. In principle, the method can be used to determine level densities up to arbitrarily high excitation energies. In practice, however, both the decreasing cross sections of isolated levels and the increasing contribution of direct reactions to these cross sections with increasing excitation energy limit the maximum excitation energy for which level densities can be determined. Level densities up to 15 MeV are observable in many nuclei; and hence, with this method, it may be possible to close the gap in level densities between the low-energy level-density measurements and the high-energy data derived from fluctuation measurements. However, as pointed out already, more measurements of cross sections to isolated levels are needed especially in energy regions where the level densities from such measurements can be compared with other independent data. Measurements of the cross sections to isolated levels reached by different particles are useful also in helping to establish the reliability of those methods for determination of level densities.

[25] E. Gadioli and L. Zetta, Phys. Rev. **167**, 1016 (1968).
[26] H. K. Vonach, R. Vandenbosch, and J. R. Huizenga, Nucl. Phys. **60**, 70 (1964).
[27] C. Bloch, Phys. Rev. **93**, 1094 (1954).
[28] N. Rosenzweig, Phys. Rev. **105**, 108 (1957).